INT. COMM. HEAT MASS TRANSFER
Vol. 17, pp. 79-91, 1990

0735-1933/90 $3.00 + .00
Printed in the United States

MASS TRANSFER ANALOGY FOR HEAT TRANSFER EXPERIMENTS IN THERMAL STORAGE

Afshin J. Ghajar, Associate Professor and **Khalid Raza**, Graduate Student
School of Mechanical and Aerospace Engineering
Oklahoma State University
Stillwater, Oklahoma 74078

(Communicated by J.P. Hartnett and W.J. Minkowycz)

ABSTRACT

The analogy between heat and mass transfer in a stratified thermal storage tank was experimentally investigated. The results indicate that it is feasible to utilize mass transfer analogy in reverse to obtain heat transfer information. However, it should be realized that mass transfer experiments tend to show less mixing than the corresponding heat transfer experiments.

Introduction

The fact that heat and mass transfer processes can be made analogous under certain specified conditions has long been established. Mass transfer analogy at times prove to be a better proposition for better understanding of complex heat transfer processes. There are situations where a mass transfer process can be set up with cleaner boundary conditions and can be studied more easily and more accurately than the corresponding heat transfer process. Moreover, mass transfer process lend itself to flow visualization through which more insight can be obtained for a corresponding heat transfer process. For the analogy to hold, the two systems for heat and mass transfer processes must have similar geometries. Physical similarity in the initial and final boundary conditions must also be fulfilled.

The purpose of this study is to investigate the analogy between heat and mass transfer experiments in a stratified thermal storage tank. In this tank both hot and cold water are stored with no physical barrier in between. Buoyancy is the only mechanism separating the hot and cold water resulting in an interface region of steep temperature gradient called thermocline. This

thermocline migrates from top to bottom (charge of hot water or discharge of cold water) or from bottom to top of the tank (discharge of hot water or charge of chilled water). There are four mechanisms contributing to the loss of stored energy in the tank. These are (1) heat loss to the ambient surroundings (2) vertical conduction in the tank wall (3) thermal diffusion in the fluid body and (4) turbulent mixing caused by introducing the fluid into the tank during both charge or discharge cycles. Several experimental studies of stratified thermal storage using hot- cold-water systems have been reported in the literature. Amongst the most recent ones are the works of Zurigat et al.[1] and Ghajar et al.[2] Few experimental studies were conducted using fresh-saline-water systems[3,4,5] as a convenient way to eliminate some of the mechanisms mentioned above, for example the first two mechanisms. However, no direct comparison of the experimental heat and mass transfer results under identical conditions have been reported in the literature in order to assess the validity of the analogy between heat and mass transfer experiments.

In this study using the procedure outlined in a later section, a direct comparison between heat and mass transfer results is provided. Experiments using fresh-saline-water to duplicate hot- cold-water experiments published earlier[1] have been conducted. To ensure geometric similarity, the same thermal storage tank used for the heat transfer experiments[1] was used for the mass transfer experiments with fresh-saline-water. It should be noted that in the heat transfer experiments the first two mechanisms, heat loss to the ambient surroundings and vertical conduction in the tank wall, contributing to heat transfer and mixing were made insignificant by using a well insulated thin wall steel tank. This leaves the thermal diffusion and turbulent mixing at the inlet as the only two mechanisms present and their effect can be studied in the mass transfer experiments. Also the same parameter variation was used for comparison purposes, which corresponds to matching of Reynolds and Richardson numbers for the heat and mass transfer experiments.

Experimental Setup

The experimental setup is shown in Fig. 1. It consists of a fresh water supply tank, a mixing tank, a catch tank, a steel test tank, metered flow system, a conductivity probe, a thermocouple probe and a data acquisition system.

The mixing tank was provided with a motor driven agitator to facilitate

in mixing while preparing a saline-water solution of a particular concentration. The test tank (16 in. dia., 56.95 in. high and 0.1 in. wall thickness) is equiped with an inlet adapter to facilitate the installation of different inlet diffusers. Two different inlet configurations were tested (see Fig. 2):

1. Perforated inlet: A perforated circular baffle (15.75 in. diameter, with 482 holes, 0.201 in. dia. each) spanning the tank cross-sectional area was installed 2.67 in. from the top of the tank. Fresh water inlet to the test tank was via a 0.709 in. inside diameter pipe.
2. Impingement inlet: A 0.709 in. inside diameter pipe entering the side of the tank and turning upwards 90° approximately 0.4 in. from the top surface of the tank with the flow impinging on the center of the top side of the tank.

In the heat transfer experiments temperature measurements were taken at nine levels along the height of the test tank using thermocouples. The test tank being initially filled with cold water and hot water pumped in. For fresh-saline water experiments a conductivity probe (Signet Scientific MK 815) was used in place of the thermocouples at the exact ninth level (lowest level in tank, 8.7 in. from bottom) to determine the concentration profile as the salt water is pushed out from the bottom of the test tank while fresh (tap) water is pumped in from the top. This flow configuration is identical to the heat transfer experiments. Since the electric conduction in aqueous solutions is temperature dependent, a thermocouple was also used at the ninth level extending 2.0 in. into the tank to monitor the solution temperature. The temperature measurements were accurate within $\pm$ 1°F.

The conductivity probe was calibrated over a range of temperatures expected to be encountered. Salt water solutions with concentrations ranging from 0.05 to 3% (by weight) were prepared in thirty five small bottles for calibration purposes. Due to the insensitivity of the conductivity probe, the mass transfer experiments were limited to a maximum concentration of 3%. The calibration temperatures were 63, 68, 77 and 86 °F. A water bath was used with a thermostatically controlled heater and pump (Lauda Circulator) to bring the solution bottles to the desired temperature before the start of calibration. The initialized probe is then immersed in each bottle, starting from the lowest in concentration and working upwards and the corresponding probe response is noted in volts. By following this procedure four calibration curves were obtained for the conductivity probe, as shown in Fig. 3.

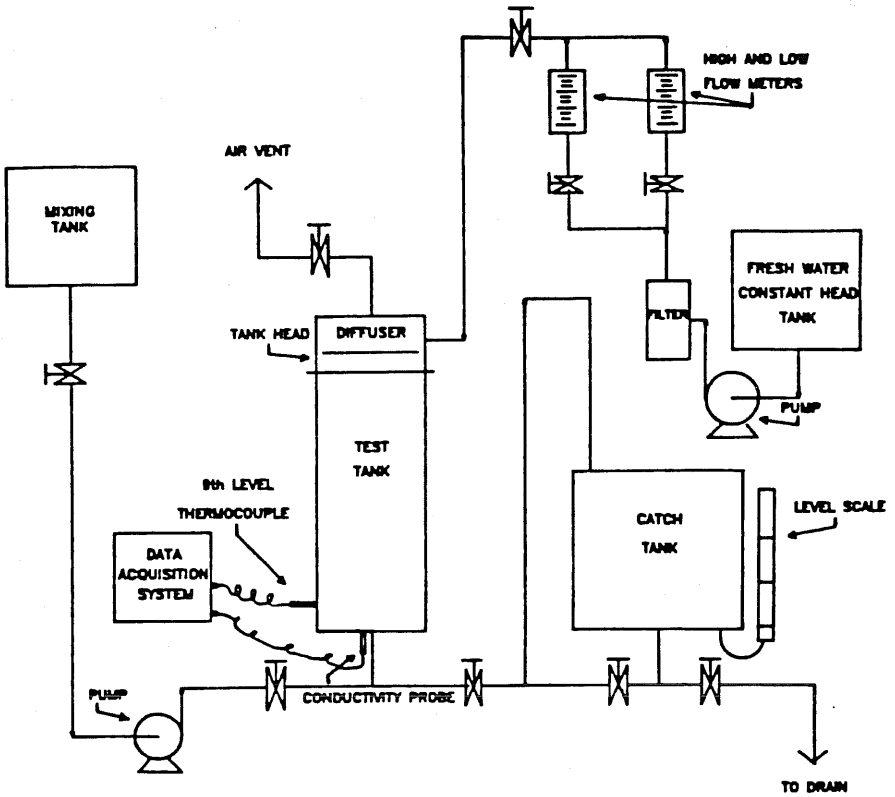

FIG. 1
Schematic of the experimental setup for fresh-saline water system.

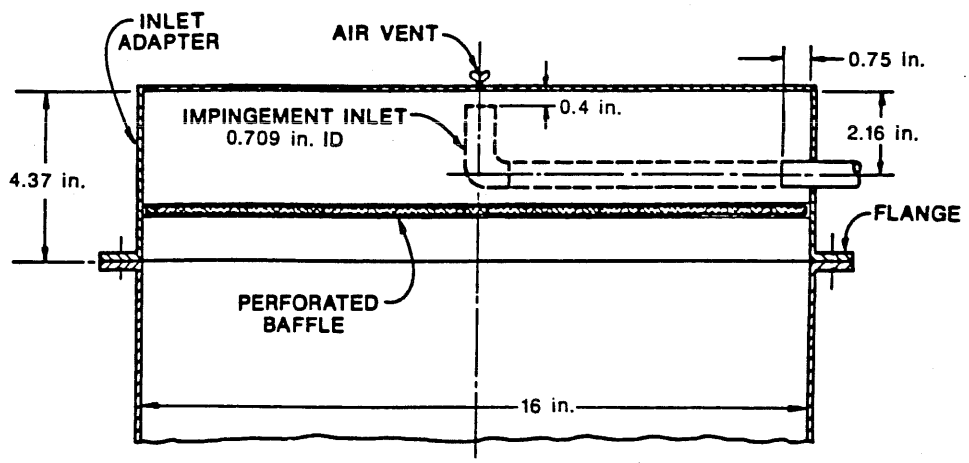

FIG. 2
Schematic of the inlet configurations tested.

Experiments With Fresh-Saline-Water System

To duplicate a heat transfer experiment (i.e., matching of Reynolds and Richardson numbers for heat and mass transfer experiments), the desired temperature difference between the tank inlet, T_{in}, and tank initial fluid temperature, T_o, for that particular test is determined first and then the corresponding density difference is obtained from the density versus temperature curve for water at atmospheric pressure. Thus where density of water as

$$\Delta\rho = |\rho(T_o) - \rho(T_{in})| \tag{1}$$

a function of temperature is obtained from the relation given in Zografos et al.[6] as

$$\rho(T) = -3.0115\times10^{-6}\ T^3 + 9.6272\times10^{-4}\ T^2 - 0.11052\ T + 1022.4 \tag{2}$$

with T expressed in Kelvin and ρ in kg/m³.

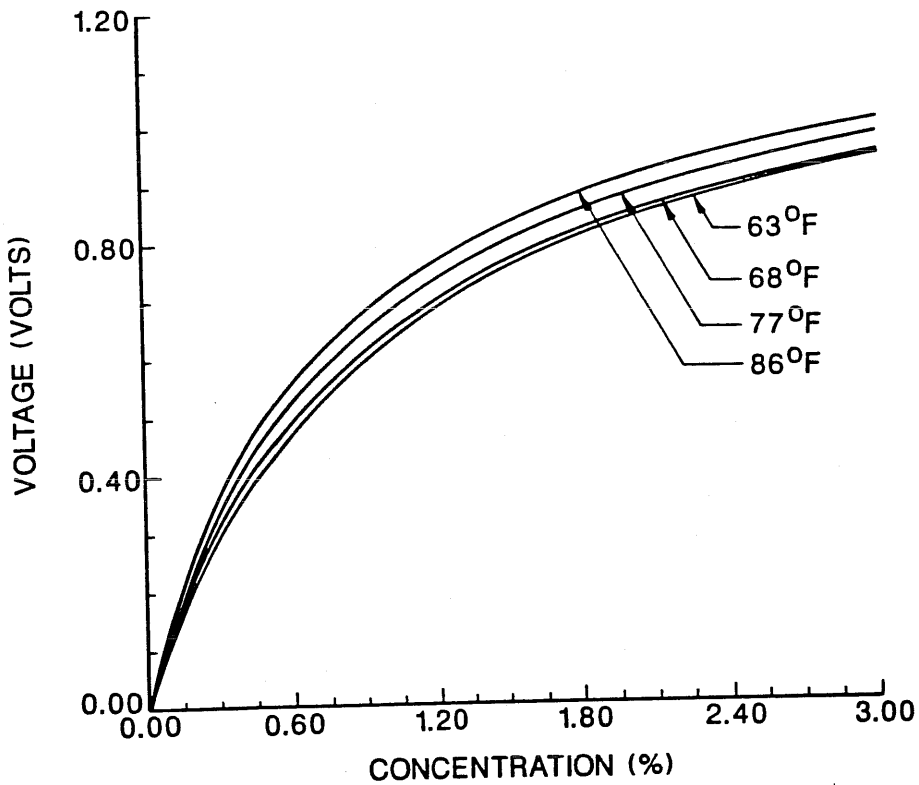

FIG. 3
Calibration profiles for conductivity probe.

The density of the saline-water needed to produce the temperature difference is then

$$\rho_{sw} = \rho_{fw} + \Delta\rho \tag{3}$$

The corresponding concentration of salt in fresh water is determined by

$$C = \left[\frac{\rho_{fw}}{\rho_{sw}} - 1\right] / \left[\frac{\rho_{fw}}{\rho_s} - 1\right] \tag{4}$$

This sets the required initial concentration of saline-water solution to be prepared in the mixing tank (see Fig. 1) by adding appropriate amount of sodium chloride as verified by the calibrated conductivity probe. It should be mentioned here that when making salt solution in the mixing tank, the temperature of water has to be noted which would determine the correct concentration made, by using the conductivity calibration data (see Fig. 3). This much information is needed before a particular test can be started. Then after obtaining the concentration data in terms of voltage it is converted to concentration using the calibration data. The saline-water density, ρ_{sw}, is then determined from Eq. (4) rearranged as

$$\rho_{sw} = \rho_{fw} / \left[1 + C \left(\frac{\rho_{fw}}{\rho_s} - 1\right)\right] \tag{5}$$

At $C = 0$, $\rho_{sw} = \rho_{fw}$ and, upon conversion to temperature, $T_{sw} = T_{fw}$. For measured concentrations ($C > 0$; $\rho_{sw} > \rho_{fw}$), the resulting temperature corresponding to ρ_{sw}, is much lower than that corresponding to ρ_{fw} and it could be in the negative region of temperatures when direct conversion of density to temperature is made. Therefore a shift in densities downward by $\Delta\rho$ is employed, where $\Delta\rho$ is given by Eq. (1). Thus an effective density is defined as

$$\rho_{eff} = \rho_{sw} - \Delta\rho \tag{6}$$

The effective density is then converted into temperature equivalent.

Using the aforementioned procedure, outlet temperature versus time curves were obtained for each experiment. A total of twelve experiments were conducted (six for each inlet configuration). The mass transfer experiments covered flow rates ranging from 1.0 to 3.36 gpm with initial salt-water concentrations varying from 1.63 to 1.95% (by weight) for the perforated inlet, and from 1.44 to 1.82% (by weight) for the impingement inlet. These concentrations corre-

spond approximately to temperature differences of 43 to 49 °F (T_o varied from 69 to 77°F) for the perforated inlet and 40 to 51 °F (T_o varied from 56 to 79°F) for the impingement inlet. The flow rate was monitored using a calibrated rotameter with full scale accuracy of ±2% and full scale repeatability of ±1%.

The data acquisition system used consists of a 40-channel Monitor Labs model 9302 data logger interfaced with a TI computer. Voltage (concentration) and temperature readings were taken at 5 to 10 second intervals. The data reduction software written in C-language and the data acquisition system are described in Rao et al.[7].

Results and Discussion

Typical mass transfer experimental results for dimensionless temperature - time profile at extreme flow rates for each of the two inlets are shown in Figs. 4 to 7 along with their corresponding heat transfer experiments[1]. From these figures it can be seen that for the inlets tested in the heat and mass transfer experiments, the thermocline has a relatively sharp gradient at the front end (hot-cold-water or salt-fresh-water interface) as opposed to the tail (the top part of thermocline in the temperature profile plots). This can be attributed to the effect of buoyancy which would be greatest at the salt-fresh-water interface (hot-cold-water interface) because the maximum difference in concentration would exist there and the greater buoyancy force would inhibit mixing.

By observing Figs. 4 to 7 for the two inlets, it can be concluded that the heat transfer temperature profiles always have lesser gradient than their corresponding mass transfer experiments. The temperature profiles obtained from mass transfer experiments tend to give less mixing than it actually exists in an actual situation of hot-cold-water system. This interesting finding can be explained on the basis of molecular mixing mechanisms that take place in heat and mass transfer experiments. In heat transfer experiments the cause of mixing at the hot and cold-water interface, in addition to the fluid churning action due to inlet disturbances, is molecular heat diffusion. In mass transfer the analogous molecular action is mass diffusion. The finding that heat transfer experiment temperature profiles have lesser gradient than their corresponding mass transfer experiment temperature profiles, suggests that the molecular heat diffusion is dominant over the mass diffusion resulting in a thicker thermocline for the corresponding heat transfer experiment. This can be supported when the value of molecular thermal diffusivity is

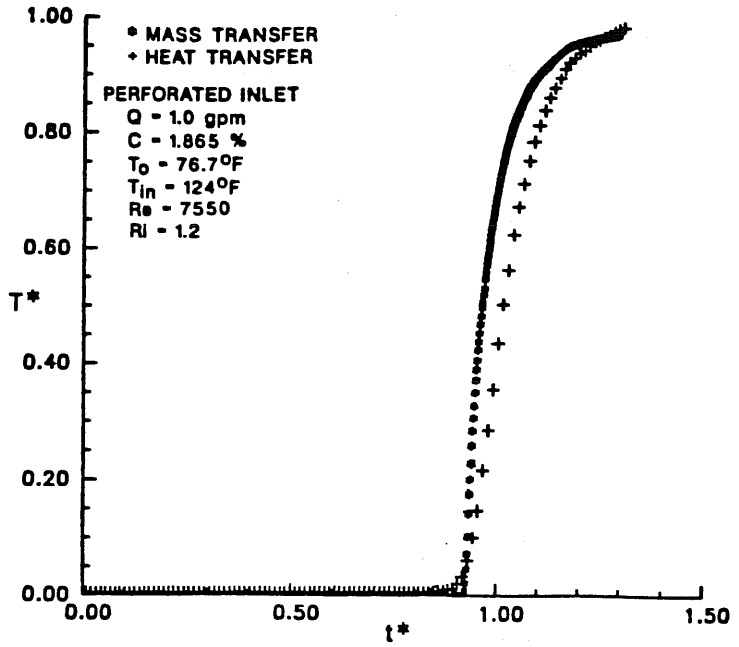

FIG. 4
Transient temperature profiles (perforated inlet, low flow rate).

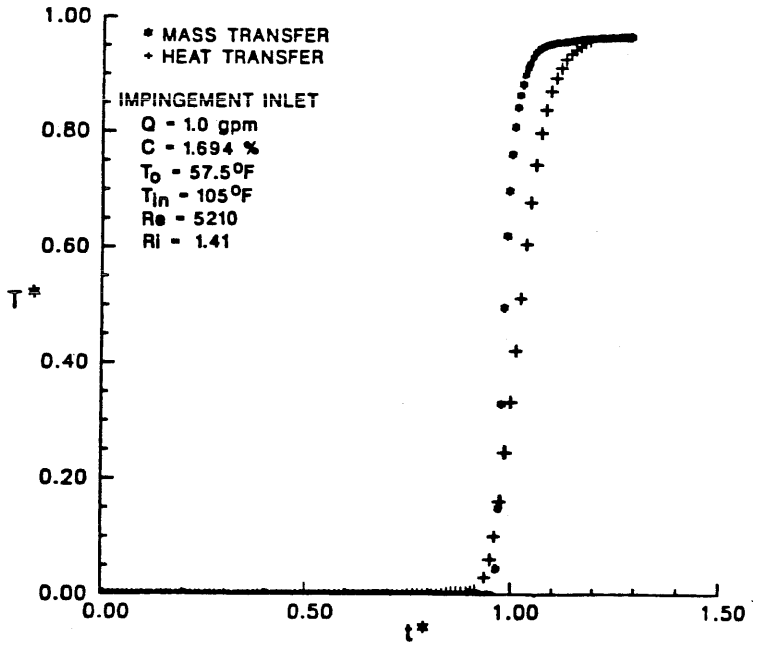

FIG. 5
Transient temperature profiles (impingement inlet, low flow rate).

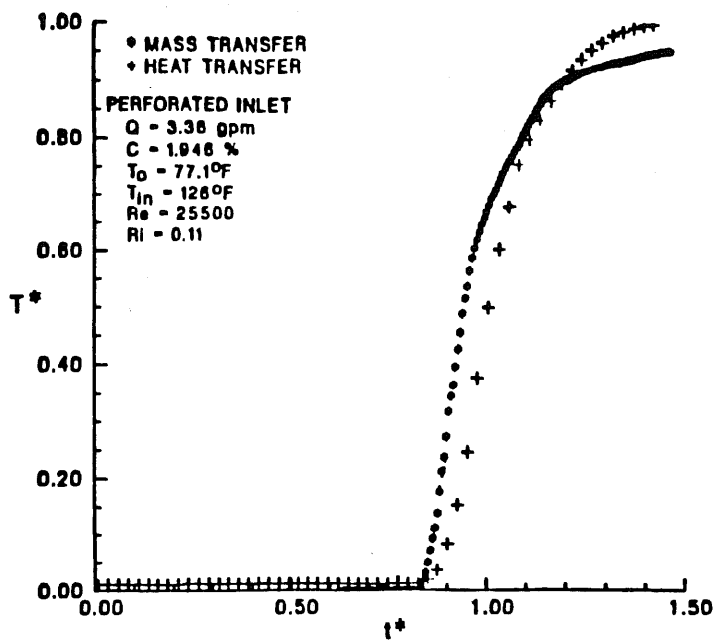

FIG. 6
Transient temperature profiles (perforated inlet, high flow rate).

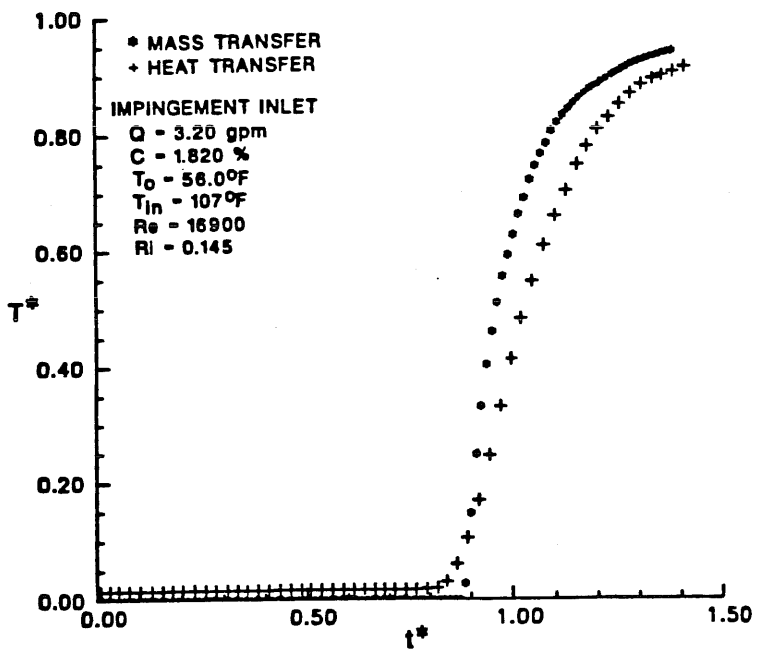

FIG. 7
Transient temperature profiles (impingement inlet, high flow rate).

compared with that of molecular mass diffusion coefficient. The value of thermal diffusivity for the temperature range encountered in the heat transfer experiments is about $6x10^{-3}$ ft^2/hr whereas, the value of diffusion coefficient for the range of salt-water concentration used in the mass transfer experiments is about $6x10^{-5}$ ft^2/hr, which is much lower than thermal diffusivity. This explains why the heat transfer temperature profiles indicate more mixing than the corresponding mass transfer experiment temperature profiles.

The influence of flow rate (Reynolds number), concentration difference (Richardson number) and inlet configuration on the temperature profile (stratification) can also be observed from Figs. 4 to 7. These figures indicate that as flow rate (Reynolds number) increases, thermocline gets thicker which indicates more mixing. However, the effect of increase in concentration difference (Richardson number) on mixing is the opposite of flow rate. That is, as concentration difference (ΔT in heat transfer experiments) increases temperature profiles become much steeper indicating less mixing. According to the heat transfer experiments values of $Ri > 1.5$ showed pronounced decrease in mixing. However, due to the limitation of the conductivity probe we were not able to duplicate the heat transfer results for $Ri > 1.5$. Finally, based on the mass transfer results presented in Figs. 4 to 7, it can be concluded that the impingement inlet performs slightly better than the perforated inlet. This observation is in agreement with the heat transfer experiments.

From the standpoint of analogy, the heat and mass transfer temperature profiles generally follow the same trend. Figures 8 and 9 give the percent difference in temperatures between the heat and mass transfer experiments for the perforated and the impingement inlets, respectively. These figures include the results of all twelve mass transfer experiments conducted in this study. The results given in Fig. 8 for the perforated inlet indicate that using mass transfer analogy, the temperature at the outlet of the storage tank can be within an error band of -6% to 22%. Similarly, from Fig. 9 for the impingement inlet, the outlet temperature can be determined within an error band of -15% to 18.5%. However, the majority of data points (85%) were within an absolute error of 10% for the perforated inlet and 91% of the data points were within an absolute error of 10% for the impingement inlet. The accuracy of the mass transfer experiments conducted was within $\pm$6%. The corresponding heat transfer experiments were obtained with an experimental error of about $\pm$8 %, which suggests that an analogy exists between the heat and mass transfer experiments.

From the results presented in Figs. 4 to 9 it can be concluded that if

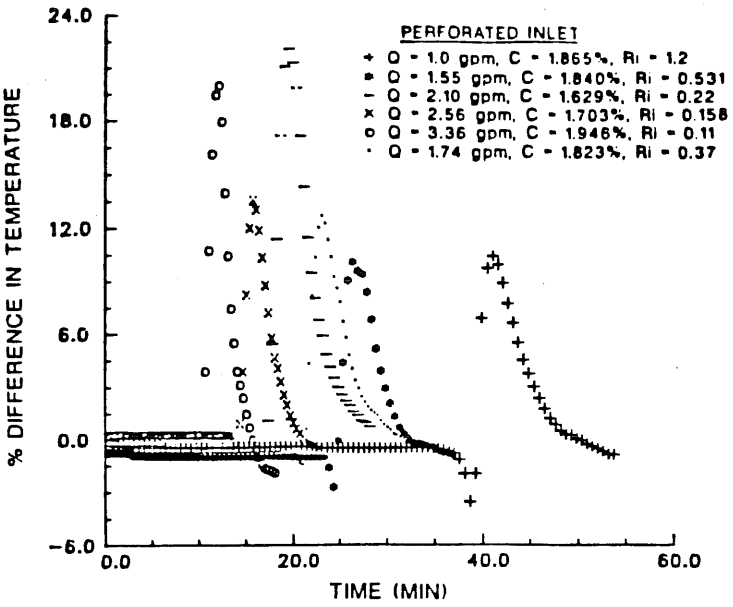

FIG. 8
Percent difference in heat and mass transfer experimental temperature profiles (perforated inlet).

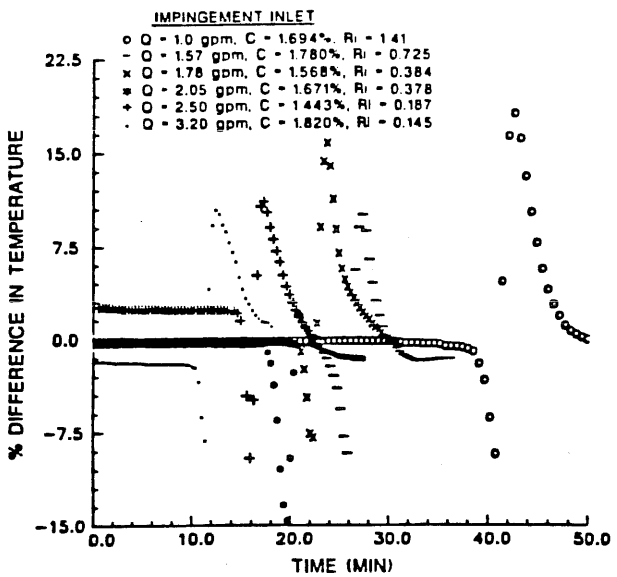

FIG. 9
Percent difference in heat and mass transfer experimental temperature profiles (impingement inlet).

mass transfer analogy is to be sought for heat transfer experiments in thermal storage, low flow rates and high Richardson numbers should be used which warrant lesser mixing and better stratification. This in turn brings the mass transfer results closer to the heat transfer results. The error associated with the analogy in such situations would be only due to the experimental error inherent in the flow system. It should be noted that in general mass transfer experiments show less mixing than there actually exist for a hot-cold-water system, and one should not be misled by this behavior.

Conclusions

The analogy between heat and mass transfer in a stratified thermal storage tank was experimentally investigated. Analysis of the mass transfer results indicate that the majority of the corresponding heat transfer results can be duplicated with an absolute error of less than 10% which is comparable to the error involved in the heat transfer experiments. From the results presented in this study it seems feasible to utilize mass transfer analogy in reverse to obtain heat transfer information through mass transfer experiments in stratified thermal storage systems. However, mass transfer experiments show less mixing than the corresponding heat transfer experiments.

Acknowledgements

This work was supported by the Oklahoma State University Center for Energy Research under grant no. 1150726. The assistance of Dr. Y. H. Zurigat with the project is gratefully acknowledged.

Nomenclature

C Concentration (percent by weight)
d Hydraulic diameter of the inlet port
g Acceleration due to gravity
H Effective height between inlet and the conductivity probe
Q Volumetric flow rate
Re Reynolds number, $Re = \rho_m V d/\mu_m$
Ri Richardson number, $Ri = \Delta\rho g H/\rho_m V^2$
T Temperature
t Time
T* Dimensionless temperature, $T^* = (T-T_{in})/(T_o-T_{in})$
t* Dimensionless time, $t^* = tV_m/H$
V Mean velocity based on inlet port area

V_m Mean vertical velocity in the tank

μ Dynamic viscosity

ρ Density

$\Delta\rho$ Density difference between the cold and hot fluids

ΔT Temperature difference between the cold and hot fluids

Subscripts

fw Fresh water

in Inlet

m Mean value

o Initial

s Salt (sodium chloride)

sw Saline water

References

1. Y. H. Zurigat, P. R. Liche, and A. J. Ghajar, Turbulent Mixing Correlations for a Thermocline Thermal Storage Tank, in S. B. Yilmaz (ed.) AIChE Symposium Series, No. 263, Vol. 84, p. 160, AIChE, New York (1988).

2. A. J. Ghajar, P. M. Moretti, and Y. H. Zurigat, Eddy Diffusivity Model for a Stratified Thermal Storage Tank, AIAA Paper No. 87-1593 presented at the AIAA 22nd Thermophysics Conference, Honolulu, Hawaii (1987).

3. Y. H. Zurigat, A. J. Ghajar, and P. M. Moretti, Applied Energy 30, 99 (1988).

4. F. J. Oppel, A. J. Ghajar, and P. M. Moretti, ASHRAE Transactions 92, 293 (1986).

5. W. D. Baines, W. W. Martin, and L. A. Sinclair, ASHRAE Transactions 88, 426 (1982).

6. A. I. Zografos, W. A. Martin, and J. E. Sunderland, Computer Methods in Applied Mechanics and Engineering 61, 177 (1987).

7. K. S. S. Rao, Y. H. Zurigat, and A. J. Ghajar, Heat Transfer Engineering 9, 58 (1988).